


A Dynamic-State Feedback Approach Employing a New State-Space Description for the Fast Wavelet Transform with Multiple Decomposition Levels

J. C. Uzinski¹  · H. M. Paiva² · R. K. H. Galvão³ · E. Assunção¹ · M. A. Q. Duarte⁴ · F. Villarreal⁵

Received: 1 August 2016 / Revised: 3 December 2016 / Accepted: 5 March 2017 / Published online: 13 March 2017
© Brazilian Society for Automatics–SBA 2017

Abstract This research paper proposes a wavelet-based dynamic-state feedback control strategy in the discrete time domain. In this proposal, the state feedback employs a state-space description for the fast wavelet transform, which is also developed in this article. The feedback gains are obtained through a linear quadratic regulator formulation, with cost weights adjusted according to suitable performance metrics. This proposal brings forward efficient results, as well as more robust systems to external perturbations and sensor noises.

Keywords State feedback control · Discrete linear quadratic regulator · Wavelet-based dynamic-state feedback

1 Introduction

Linear quadratic regulator (LQR) is an automated way of finding an appropriate state feedback controller, which has been used in various applications (Zhang and Fu 1996; Fernando and Kumarawadu 2015; Pradhan and Ghosh 2015; Liu

et al. 2013; Zhang et al. 2014). The LQR provides a key role in many control design methods. Besides being a powerful design method, it is in many aspects the principle of several current systematic control design procedures. Both the linear quadratic Gaussian or H_2 , and H_∞ controller design procedures have usage and philosophy similar to the LQR methodology (Lublin and Athans 1996; Maccari et al. 2014).

Improving stability margins via dynamic-state feedback for systems is well studied in Zhang and Fu (1996), Schmitendorf and Stalford (1997), Holmberg et al. (2001), Ulsoy (2013), Ulsoy (2015) and Verdea et al. (2013). By analyzing robustness properties of the LQR, in Schmitendorf and Stalford (1997), Holmberg et al. (2001), it has shown that the guaranteed gain/phase margins of LQR need to be carefully interpreted. This analysis leads to the discussion of using dynamic-state feedback. Furthermore, the stability margin for a linear system with constant uncertainty can be increased beyond that attainable by a static-state feedback with the use of a dynamic-state feedback controller (Zhang and Fu 1996).

In this paper, a dynamic-state feedback control approach employing a new state-space description for the multi-level fast wavelet transform (FWT) is proposed. The main characteristic that makes the proposed approach efficient and easy to implement is the use of the standard discrete linear quadratic regulator. This proposal is justified by the fact of getting more robust systems resistant to perturbations and measuring noise.

The state-space description mentioned is developed from a previous paper that presents the state-space description for single-level decomposition of the FWT algorithm (Uzinski et al. 2015). In the state-space description for the entire filter bank with M decomposition levels, the outputs are the approximation in the last level and the details in all levels as in the FWT algorithm. The main characteristics presented by the single-level formulation are carried to the descrip-

✉ J. C. Uzinski
juliouszinski@aluno.feis.unesp.br

¹ São Paulo State University (Unesp), School of Engineering, Ilha Solteira, São Paulo, Brazil

² Institute of Science and Technology (ICT), Universidade Federal de São Paulo - UNIFESP, São José dos Campos, São Paulo, Brazil

³ Department of Electronic Engineering - ITA, São José dos Campos, São Paulo, Brazil

⁴ Department of Mathematics - UEMS, Universidade Estadual de Mato Grosso do Sul, Cassilândia, Mato Grosso do Sul, Brazil

⁵ Department of Mathematics - FEIS, Universidade Estadual Paulista - UNESP, Ilha Solteira, São Paulo, Brazil

tion for multi-level decomposition, as the explicit presence of parameters that can be freely adjusted holding the guarantees of perfect reconstruction and orthogonality. The state-space realization proposed to represent the filter bank with M levels is controllable and observable.

The paper is organized into three main parts: Sect. 2 deals with the development of the state-space for multi-level wavelet filter bank and its background, Sect. 3 presents the proposed dynamic-state feedback approach, and Sect. 4 contains results and analysis.

2 State-Space for Multi-Level FWT

2.1 On the Space of Orthonormal Wavelets

By adapting the work of Vaidyanathan (1993) on the factorization of paraunitary matrices and parameterizing the space of orthonormal wavelets by a set of angular parameters, Sherlock and Monro (1998) devised a simple and elegant framework to parameterize the space of orthonormal wavelets by a set of angular parameters (Paiva et al. 2009; Paiva and Galvão 2012). Sherlock and Monro’s formulation is presented in the following.

Let $H^{(N)}(z)$ and $G^{(N)}(z)$ be the transfer functions of the low-pass and high-pass filters, respectively, for an orthonormal filter bank with length- $2N$, such that

$$H^{(N)}(z) = \sum_{i=0}^{2N-1} h_i^{(N)} z^{-i} \tag{1}$$

and

$$G^{(N)}(z) = \sum_{i=0}^{2N-1} g_i^{(N)} z^{-i}, \tag{2}$$

where

$$g_i^{(N)} = (-1)^{i+1} h_{2N-1-i}^{(N)}, \quad i = 0, 1, \dots, 2N - 1, \tag{3}$$

and

$$\begin{aligned} h_0^1 &= \cos(\alpha_1) \\ h_1^1 &= \sin(\alpha_1) \\ h_0^{N+1} &= \cos(\alpha_{N+1})h_0^N \\ h_{2i}^{N+1} &= \cos(\alpha_{N+1})h_{2i}^N - \sin(\alpha_{N+1})h_{2i-1}^N, \\ h_{2N}^{N+1} &= -\sin(\alpha_{N+1})h_{2N-1}^N \\ h_1^{N+1} &= \sin(\alpha_{N+1})h_0^N \\ h_{2i+1}^{N+1} &= \sin(\alpha_{N+1})h_{2i}^N + \cos(\alpha_{N+1})h_{2i-1}^N, \\ h_{2N+1}^{N+1} &= \cos(\alpha_{N+1})h_{2N-1}^N \end{aligned} \tag{4}$$

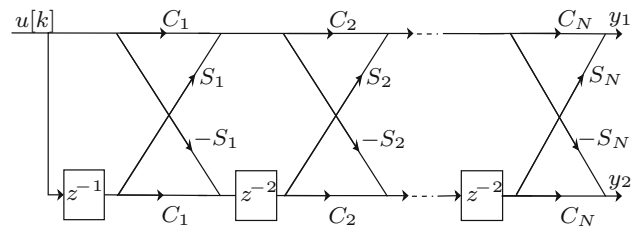


Fig. 1 A DWT decomposition level represented by a lattice structure. Adapted from Akansu and Haddad (2001)

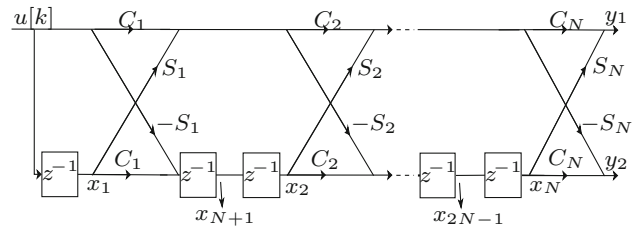


Fig. 2 Parameterization of the filter bank in the state-space. Adapted from Uzinski et al. (2015)

with $i = 0, 1, \dots, N - 1$. In (4), $\alpha = [\alpha_1 \alpha_2 \dots \alpha_N]$ is the angular parameter set, following the notation defined in the original work of Sherlock and Monro (1998.)

Let $u[k]$ be an input signal processed in a level of the discrete wavelet transform (DWT). It has two outputs, y_1 and y_2 corresponding to the input signal filtered by the low-pass filter and by the high-pass filter, respectively. This filtering process for one decomposition level can be seen through the implementation of these filters in lattice structure, Fig. 1.

In Fig. 1, symbols C_i and S_i denote $\sin(\theta_i)$ and $\cos(\theta_i)$, respectively, where $\theta = [\theta_1 \theta_2 \dots \theta_N]$ and $\theta_1 = \alpha_N, \theta_2 = \alpha_{N-1}, \dots, \theta_N = \alpha_1$.

2.2 A State-Space Description for One Single Decomposition Level of a Wavelet Filter Bank

According to Uzinski et al. (2015), the model for a single-level in the state-space takes the form

$$\mathbf{x}[k + 1] = \mathbf{A}\mathbf{x}[k] + \mathbf{B}\mathbf{u}[k] \tag{5}$$

$$\mathbf{y}[k] = \mathbf{C}\mathbf{x}[k] + \mathbf{D}\mathbf{u}[k]. \tag{6}$$

where $\mathbf{x} = [x_1 \ x_2 \ \dots \ x_{2N-1}]^T$ and k denotes the k th sampling instant. This state-space description was obtained through the procedure shown in Fig. 2.

In (5) and (6), \mathbf{A} , \mathbf{B} , \mathbf{C} and \mathbf{D} are given by (7), (8), (9) and (10), respectively.

$$\mathbf{A} = \begin{bmatrix} 0 & 0 & 0 & \cdots & 0 & 0 & 0 & 0 & \cdots & 0 \\ 0 & 0 & 0 & \cdots & 0 & 0 & 1 & 0 & \cdots & 0 \\ 0 & 0 & 0 & \cdots & 0 & 0 & 0 & 1 & \cdots & 0 \\ 0 & 0 & 0 & \cdots & 0 & 0 & 0 & 0 & 1 & \cdots & 0 \\ \vdots & \vdots & \vdots & \ddots & \vdots & \vdots & \vdots & \vdots & \vdots & \ddots & \vdots \\ 0 & 0 & 0 & \cdots & 0 & 0 & 0 & 0 & \cdots & 1 \\ C_1 & 0 & 0 & \cdots & 0 & 0 & 0 & 0 & \cdots & 0 \\ -S_2 S_1 & C_2 & 0 & \cdots & 0 & 0 & 0 & 0 & \cdots & 0 \\ -S_3 C_2 S_1 & -S_3 S_2 & C_3 & \cdots & 0 & 0 & 0 & 0 & \cdots & 0 \\ \vdots & \vdots & \vdots & \ddots & \vdots & \vdots & \vdots & \vdots & \vdots & \ddots & \vdots \\ S_{N-1} S_1 \prod_{i=2}^{N-2} C_i & S_{N-1} S_2 \prod_{i=3}^{N-2} C_i & S_{N-1} S_3 \prod_{i=4}^{N-2} C_i & \cdots & C_{N-1} & 0 & 0 & 0 & \cdots & 0 \end{bmatrix}, \tag{7}$$

$$\mathbf{B} = \begin{bmatrix} 1 \\ 0 \\ \vdots \\ 0 \\ -S_1 \\ -S_2 C_1 \\ \vdots \\ -S_{N-1} \prod_{i=1}^{N-2} C_i \end{bmatrix}. \tag{8}$$

$$\mathbf{C} = \begin{bmatrix} S_1 \prod_{i=2}^N C_i & S_2 \prod_{i=3}^N C_i & \cdots & S_{N-2} \prod_{i=N-1}^N C_i & S_{N-1} C_N & S_N & 0 & \cdots & 0 \\ -S_N S_1 \prod_{i=2}^{N-1} C_i & -S_N S_2 \prod_{i=3}^{N-1} C_i & \cdots & -S_N S_{N-2} \prod_{i=N-1}^{N-1} C_i & -S_N S_{N-1} & C_N & 0 & \cdots & 0 \end{bmatrix} \tag{9}$$

$$\mathbf{D} = \begin{bmatrix} \prod_{i=1}^N C_i \\ -S_N \prod_{i=1}^{N-1} C_i \end{bmatrix}, \tag{10}$$

The sizes of matrices **A**, **B**, **C** and **D** are $(2N - 1) \times (2N - 1)$, $(2N - 1) \times 1$, $2 \times (2N - 1)$ and 2×1 , respectively. An important feature of this realization (**A**, **B**, **C**, **D**) is that it is minimal, namely reachable and observable. Further discussions, proof and illustrative examples can be found in [Uzinski et al. \(2015\)](#).

2.3 Wavelet Filter Bank and the *Algorithme à Trous*

After recalling the theory about the parameterization for the *i*th decomposition level, it is necessary to show how the fast wavelet transform (FWT) works. This method uses digital filter banks in a tree structure, as shown as an example with

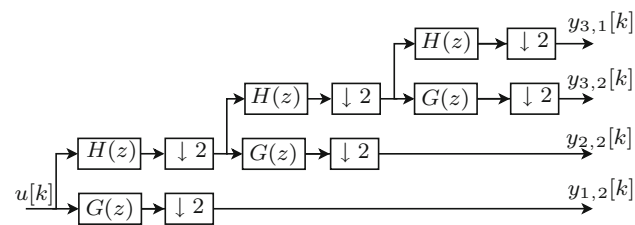


Fig. 3 Three-level binary tree-structured quadrature mirror filter (QMF) bank. Adapted from [Vaidyanathan \(1993\)](#)

three decomposition levels, in [Fig. 3](#). In this figure, $H(z)$ and $G(z)$ indicate the low-pass and high-pass filters and $\downarrow 2$ denotes the downsampling operators ([Vaidyanathan 1993](#)).

An equivalent implementation for the FWT, [Fig. 3](#), avoiding the downsampling operations in each decomposition level is the *Algorithme à Trous* (algorithm with “holes”) ([Vetterli and Kovačević 1995](#)), [Fig. 4](#).

As stated by [Paiva \(2005\)](#), [Vetterli and Kovačević \(1995\)](#), the relationship between the coefficients $y_i[k]$ (FWT) and $\underline{y}_i[k]$ (*Algorithme à Trous*) is

$$y_i[k] = (\downarrow 2^i) \underline{y}_i[k]. \tag{11}$$

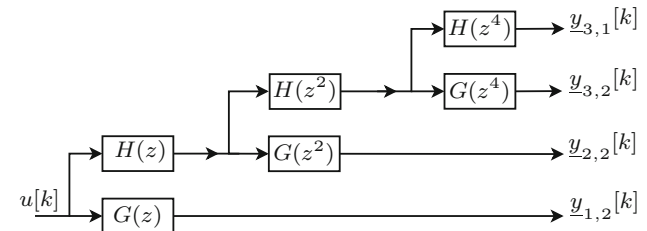


Fig. 4 Equivalent filter bank to the one in [Fig. 3](#) using the *Algorithme à Trous*. Adapted from [Vetterli and Kovačević \(1995\)](#)

The *Algorithme à Trous* is used in the new state-space description for the multi-level FWT proposed in this paper.

2.4 The State-Space Parameterization for Multiple Decomposition Levels

In this subsection, the parameterization for one single decomposition level of a wavelet filter bank presented in Uzinski et al. (2015) is extended for M decomposition levels of a perfect-reconstruction wavelet filter bank, which is known as fast wavelet transform. The *Algorithme à Trous*, which was described in Sect. 2.3, was adopted to overcome the difficulties associated with the downsampling operations.

The state vector associated with the lattice in the i th decomposition level has $2N - 1$ states and it is denoted by

$$\mathbf{x}_i[k] = \begin{bmatrix} x_{i,1}[k] \\ x_{i,2}[k] \\ x_{i,3}[k] \\ \vdots \\ x_{i,2N-1}[k] \end{bmatrix}, \tag{12}$$

the output in the i th decomposition level with $\underline{y}_{i,1}[k]$ and $\underline{y}_{i,2}[k]$ associated with the low-pass and high-pass channels, respectively, by

$$\underline{\mathbf{y}}_i[k] = \begin{bmatrix} \underline{y}_{i,1}[k] \\ \underline{y}_{i,2}[k] \end{bmatrix}, \tag{13}$$

and the matrices \mathbf{C} and \mathbf{D} are conveniently rewritten as

$$\mathbf{C} = \begin{bmatrix} \mathbf{C}_1 \\ \mathbf{C}_2 \end{bmatrix}$$

and

$$\mathbf{D} = \begin{bmatrix} D_1 \\ D_2 \end{bmatrix}.$$

The state-space description for a single decomposition level i of a wavelet filter bank as previously presented and its denotations are shown in Fig. 5.

In Fig. 5, the input $\underline{y}_{i-1,1}[k]$ at level i is the low-pass output at the level $i - 1$. The elements $\mathbf{x}_i[k]$, $\underline{y}_{i,1}[k]$ and $\underline{y}_{i,2}[k]$ are the state variable and two outputs in the i th decomposition level (algorithm with “holes”), respectively.

By considering the state-space description for the i th decomposition level and recalling the *Algorithme à Trous*, the lattice model in the first decomposition level has the form

$$\mathbf{x}_1[k + 1] = \mathbf{A}\mathbf{x}_1[k] + \mathbf{B}u[k], \tag{14}$$

$$\underline{\mathbf{y}}_1[k] = \begin{bmatrix} \mathbf{C}_1 \\ \mathbf{C}_2 \end{bmatrix} \mathbf{x}_1[k] + \begin{bmatrix} D_1 \\ D_2 \end{bmatrix} u[k], \tag{15}$$

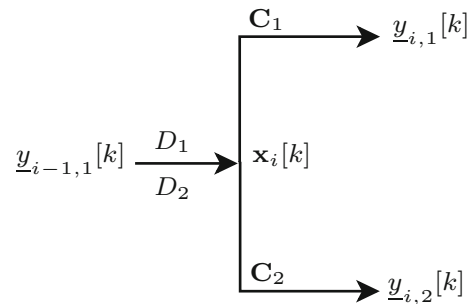


Fig. 5 Representation of the state-space description for a single decomposition level i of a wavelet filter bank

while for $i > 1$ it is

$$\mathbf{x}_i[k + 2^{i-1}] = \mathbf{A}\mathbf{x}_i[k] + \mathbf{B}\underline{y}_{i-1,1}[k], \tag{16}$$

$$\underline{\mathbf{y}}_i[k] = \begin{bmatrix} \mathbf{C}_1 \\ \mathbf{C}_2 \end{bmatrix} \mathbf{x}_i[k] + \begin{bmatrix} D_1 \\ D_2 \end{bmatrix} \underline{y}_{i-1,1}[k]. \tag{17}$$

The *Algorithme à Trous* (Fig. 4) employs filters of the form $H(z^2)$, $H(z^4)$, $H(z^8)$ and so on. It should be noted that $H(z^2)$ is twice as longer as $H(z)$. This difference in the filter length is taken into account in (16). In fact, to understand this point, consider $i = 2$ in (16). In this case

$$\mathbf{x}_2[k + 2] = \mathbf{A}\mathbf{x}_2[k] + \mathbf{B}\underline{y}_{1,1}[k]. \tag{18}$$

Considering an additional state vector $\mathbf{w}[k] = \mathbf{x}_2[k + 1]$, (18) could be rewritten as

$$\mathbf{w}[k + 1] = \mathbf{A}\mathbf{x}_2[k] + \mathbf{B}\underline{y}_{1,1}[k] \tag{19}$$

$$\mathbf{x}_2[k + 1] = \mathbf{w}[k], \tag{20}$$

that is:

$$\begin{bmatrix} \mathbf{w} \\ \mathbf{x}_2 \end{bmatrix} [k + 1] = \begin{bmatrix} 0 & \mathbf{A} \\ \mathbf{I} & 0 \end{bmatrix} \begin{bmatrix} \mathbf{w} \\ \mathbf{x}_2 \end{bmatrix} [k] + \begin{bmatrix} \mathbf{B} \\ 0 \end{bmatrix} \underline{y}_{1,1}[k], \tag{21}$$

where \mathbf{I} is an identity matrix and 0 is a null matrix. Therefore, using $\mathbf{x}_2[k + 2]$ in (16) is equivalent to using more states to describe a longer filter. For $i = 2$, $\mathbf{x}_2[k + 2]$ it is necessary to use twice as many states. For $i = 3$, $\mathbf{x}_3[k + 4]$ it means that four times as many states are necessary and so on.

Taking the entire analysis filter bank, the following state vector can be defined as the filter bank with M decomposition levels, Fig. 6,

$$\mathbf{x}[k] = \begin{bmatrix} \mathbf{x}_1[k] \\ \mathbf{x}_2[k] \\ \mathbf{x}_3[k] \\ \vdots \\ \mathbf{x}_M[k] \end{bmatrix}. \tag{22}$$

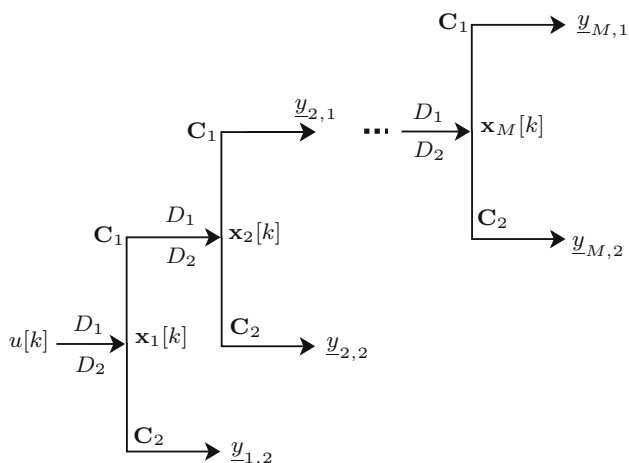


Fig. 6 Wavelet filter bank with M decomposition levels seen as state-space description

When the “holes” are considered, the equation for the filter bank can be written as

$$\begin{bmatrix} \mathbf{x}_1[k + 1] \\ \mathbf{x}_2[k + 2] \\ \vdots \\ \mathbf{x}_M[k + 2^{M-1}] \end{bmatrix} = \begin{bmatrix} \mathbf{A}\mathbf{x}_1[k] + \mathbf{B}u[k] \\ \mathbf{A}\mathbf{x}_2[k] + \mathbf{B}y_{1,1}[k] \\ \vdots \\ \mathbf{A}\mathbf{x}_M[k] + \mathbf{B}y_{M-1,1}[k] \end{bmatrix},$$

then

$$\begin{bmatrix} \mathbf{x}_1[k + 1] \\ \mathbf{x}_2[k + 2] \\ \vdots \\ \mathbf{x}_M[k + 2^{M-1}] \end{bmatrix} = \begin{bmatrix} \mathbf{A} & 0 & \cdots & 0 \\ \mathbf{B}\mathbf{C}_1 & \mathbf{A} & \cdots & 0 \\ \vdots & \vdots & \ddots & \vdots \\ \mathbf{B}D_1^{M-2}\mathbf{C}_1 & \cdots & \mathbf{B}\mathbf{C}_1 & \mathbf{A} \end{bmatrix} \begin{bmatrix} \mathbf{x}_1[k] \\ \mathbf{x}_2[k] \\ \vdots \\ \mathbf{x}_M[k] \end{bmatrix} + \begin{bmatrix} \mathbf{B} \\ \mathbf{B}D_1 \\ \vdots \\ \mathbf{B}D_1^{M-1} \end{bmatrix} u[k]. \tag{23}$$

Let $\underline{\mathbf{y}}[k]$ be the output vector, comprising the approximation in the last level and details in all levels, defined as

$$\underline{\mathbf{y}}[k] = \begin{bmatrix} y_{M,1}[k] \\ y_{M,2}[k] \\ y_{M-1,2}[k] \\ \vdots \\ y_{1,2}[k] \end{bmatrix}, \tag{24}$$

the output equation can be finally written for the filter bank as follows:

$$\underline{\mathbf{y}}[k] = \begin{bmatrix} \mathbf{C}_1\mathbf{x}_M[k] + D_1y_{M-1,1}[k] \\ \mathbf{C}_2\mathbf{x}_M[k] + D_2y_{M-1,1}[k] \\ \mathbf{C}_2\mathbf{x}_{M-1}[k] + D_2y_{M-2,1}[k] \\ \vdots \\ \mathbf{C}_2\mathbf{x}_1[k] + D_2u[k] \end{bmatrix},$$

thus

$$\begin{bmatrix} y_{M,1}[k] \\ y_{M,2}[k] \\ y_{M-1,2}[k] \\ \vdots \\ y_{1,2}[k] \end{bmatrix} = \begin{bmatrix} D_1^{M-1}\mathbf{C}_1 & \cdots & D_1^2\mathbf{C}_1 & D_1\mathbf{C}_1 & \mathbf{C}_1 \\ D_2D_1^{M-2}\mathbf{C}_1 & \cdots & D_2D_1\mathbf{C}_1 & D_2\mathbf{C}_1 & \mathbf{C}_2 \\ D_2D_1^{M-3}\mathbf{C}_1 & \cdots & D_2\mathbf{C}_1 & \mathbf{C}_2 & 0 \\ \vdots & \ddots & \vdots & \vdots & \vdots \\ \mathbf{C}_2 & \cdots & 0 & 0 & 0 \end{bmatrix} \begin{bmatrix} \mathbf{x}_1[k] \\ \mathbf{x}_2[k] \\ \mathbf{x}_3[k] \\ \vdots \\ \mathbf{x}_M[k] \end{bmatrix} + \begin{bmatrix} D_1^M \\ D_2D_1^{M-1} \\ D_2D_1^{M-2} \\ \vdots \\ D_2 \end{bmatrix} u[k]. \tag{25}$$

After all, the version to Fig. 5 for the M decomposition levels proposal, as previously obtained, is presented in Fig. 6.

However, (23) is not the state equation for multi-level FWT, some changes are required, and changes in (23) will imply other changes in (25).

Suitably defining

$$\begin{cases} x_{M+1}[k] = x_2[k + 1], \\ x_{M+2}[k] = x_3[k + 1], \\ x_{M+3}[k] = x_{M+2}[k + 1], \\ x_{M+4}[k] = x_{M+3}[k + 1], \\ x_{M+5}[k] = x_4[k + 1], \\ x_{M+6}[k] = x_{M+5}[k + 1], \\ \vdots \\ x_{M+11}[k] = x_{M+10}[k + 1], \\ \vdots \\ x_{M+\varepsilon+1}[k] = x_M[k + 1], \\ x_{M+\varepsilon+2}[k] = x_{M+\varepsilon+1}[k + 1], \\ \vdots \\ x_{M+\varepsilon+2^{M-1}-1}[k] = x_{M+\varepsilon+2^{M-1}-2}[k + 1], \end{cases} \tag{26}$$

where $\varepsilon = \sum_{i=2}^{M-1} [2^{i-1} - 1]$, hence

$$\begin{cases} x_{M+1}[k+1] = x_2[k+2], \\ x_{M+4}[k+1] = x_3[k+4], \\ x_{M+11}[k+1] = x_4[k+8], \\ \vdots \\ x_{M+\varepsilon+2^{M-1}-1}[k+1] = x_M[k+2^{M-1}]. \end{cases}$$

In this way, vector $\mathbf{x}[k]$ becomes

$$\mathbf{x}[k] = \begin{bmatrix} \mathbf{x}_1[k] \\ \mathbf{x}_2[k] \\ \vdots \\ \mathbf{x}_M[k] \\ \mathbf{x}_{M+1}[k] \\ \mathbf{x}_{M+2}[k] \\ \vdots \\ \mathbf{x}_\eta[k] \end{bmatrix}, \tag{28}$$

with $\eta = M + \sum_{i=2}^{M-1} [2^{i-1} - 1] + 2^{M-1} - 1$, namely, $\eta = M + \varepsilon + 2^{M-1} - 1$.

Matrices of the state-space realization for M decomposition levels are denoted as $\mathbf{A}_M, \mathbf{B}_M, \mathbf{C}_M$ and \mathbf{D}_M .

From (23), (25), (26) and (27), matrix \mathbf{A}_M takes the form

$$\mathbf{A}_M = \begin{bmatrix} \mathbf{A} & 0 & \dots & 0 & 0 & 0 & \dots & 0 \\ 0 & 0 & \dots & 0 & \mathbf{I} & 0 & \dots & 0 \\ \vdots & \vdots & \ddots & \vdots & \vdots & \vdots & \ddots & \vdots \\ \mathbf{BC}_1 & \mathbf{A} & \dots & 0 & 0 & 0 & \dots & 0 \\ 0 & 0 & \dots & 0 & 0 & \mathbf{I} & \dots & 0 \\ \vdots & \vdots & \ddots & \vdots & \vdots & \vdots & \ddots & \vdots \\ 0 & 0 & \dots & 0 & 0 & 0 & \dots & \mathbf{I} \\ \mathbf{BD}_1^{M-2}\mathbf{C}_1 & \mathbf{BD}_1^{M-3}\mathbf{C}_1 & \dots & \mathbf{A} & 0 & 0 & \dots & 0 \end{bmatrix}, \tag{29}$$

where \mathbf{I} is the $(2N - 1) \times (2N - 1)$ identity matrix. In the same way, each element denoted by 0 is a $(2N - 1) \times (2N - 1)$ null matrix. While \mathbf{B}_M is defined as

$$\mathbf{B}_M = \begin{bmatrix} \mathbf{B} \\ 0 \\ \vdots \\ \mathbf{BD}_1 \\ 0 \\ \vdots \\ 0 \\ \mathbf{BD}_1^{M-1} \end{bmatrix}, \tag{30}$$

with 0 being a $(2N - 1) \times 1$ null vector. Matrix \mathbf{C}_M is given by

$$\mathbf{C}_M = \begin{bmatrix} D_1^{M-1}\mathbf{C}_1 & \dots & D_1^2\mathbf{C}_1 & D_1\mathbf{C}_1 & \mathbf{C}_1 & 0 & \dots & 0 \\ D_2D_1^{M-2}\mathbf{C}_1 & \dots & D_2D_1\mathbf{C}_1 & D_2\mathbf{C}_1 & \mathbf{C}_2 & 0 & \dots & 0 \\ D_2D_1^{M-3}\mathbf{C}_1 & \dots & D_2\mathbf{C}_1 & \mathbf{C}_2 & 0 & 0 & \dots & 0 \\ \vdots & \ddots & \vdots & \vdots & \vdots & \ddots & \vdots & \vdots \\ \mathbf{C}_2 & \dots & 0 & 0 & 0 & 0 & \dots & 0 \end{bmatrix}, \tag{31}$$

with 0 being an $1 \times (2N - 1)$ null vector. Vector \mathbf{D}_M is equal to

$$\mathbf{D}_M = \begin{bmatrix} D_1^M \\ D_2D_1^{M-1} \\ D_2D_1^{M-2} \\ \vdots \\ D_2 \end{bmatrix}. \tag{32}$$

Finally, matrices (29), (30), (31) and (32) are the description in the state-space for analysis wavelet FIR filter banks with multiple decomposition levels. This proposal is based on *Algorithme à Trous*; therefore, it is necessary to remember that the relationship among the coefficients $\mathbf{y}_i[k]$ (FWT) and $\mathbf{y}_i[k]$ (*Algorithme à Trous*) is given by (11); in other words, the convenient decimation must be done after state-space description.

Dimensions of the matrices in the state-space description are:

- $\dim(\mathbf{A}_M) = \eta(2N - 1) \times \eta(2N - 1)$;
- $\dim(\mathbf{B}_M) = \eta(2N - 1) \times 1$;
- $\dim(\mathbf{C}_M) = (M + 1) \times \eta(2N - 1)$;
- $\dim(\mathbf{D}_M) = (M + 1) \times 1$,

and if $\mathcal{R}_{\mathbf{A}_M}, \mathbf{B}_M$ and $\mathcal{S}_{\mathbf{C}_M}, \mathbf{A}_M$ are respectively controllability and observability matrices, then

- $\dim(\mathcal{R}_{\mathbf{A}_M}, \mathbf{B}_M) = \eta(2N - 1) \times \eta(2N - 1)$;
- $\dim(\mathcal{S}_{\mathbf{C}_M}, \mathbf{A}_M) = (M + 1)\eta(2N - 1) \times \eta(2N - 1)$.

An important result about the state-space description is the minimality condition, which is the combination of controllability and observability conditions. For $M = 1$, the proposed state-space description is minimal, and this can be checked in [Uzinski et al. \(2015\)](#). For an arbitrary M , the minimality condition is exploited in Theorem 2. The proof of this theorem is made by using mathematical induction. For this reason, Lemma 1 states that the proposed state-space description is minimal for $M = 2$ (for $M = 1$ there is no delay operators included in the parameterization).

Lemma 1 A realization $(\mathbf{A}_M, \mathbf{B}_M, \mathbf{C}_M, \mathbf{D}_M)$ for $M = 2$ given by (29), (30), (31) and (32), respectively, with all angles different from $0, \pi/2, \pi$ and $3\pi/2$ ¹, is minimal.

Proof For $M = 2$ matrices $\mathbf{A}_M, \mathbf{B}_M$ and \mathbf{C}_M become

$$\mathbf{A}_M = \begin{bmatrix} \mathbf{A} & 0 & 0 \\ 0 & 0 & \mathbf{I} \\ \mathbf{BC}_1 & \mathbf{A} & 0 \end{bmatrix}, \tag{33}$$

$$\mathbf{B}_M = \begin{bmatrix} \mathbf{B} \\ 0 \\ \mathbf{BD}_1 \end{bmatrix} \tag{34}$$

and

$$\mathbf{C}_M = \begin{bmatrix} D_1\mathbf{C}_1 & \mathbf{C}_1 & 0 \\ \mathbf{C}_2\mathbf{C}_1 & \mathbf{C}_2 & 0 \\ \mathbf{C}_2 & 0 & 0 \end{bmatrix}. \tag{35}$$

By the mathematical induction principle, it is necessary to verify that the lemma is true for $N = 1$ and if it holds for a certain N this implies that it will be true for $N + 1$. It is made as follows.

- For $N = 1$: $\mathbf{A} = 0, \mathbf{B} = 1, \mathbf{C} = [S_1 \ C_1]^T$ and $\mathbf{D} = [C_1 \ S_1]^T$. By replacing these values in (33), (34) and (35):

$$\mathbf{A}_M = \begin{bmatrix} 0 & 0 & 0 \\ 0 & 0 & 1 \\ S_1 & 0 & 0 \end{bmatrix}, \quad \mathbf{B}_M = \begin{bmatrix} 1 \\ 0 \\ C_1 \end{bmatrix}$$

$$\text{and } \mathbf{C}_M = \begin{bmatrix} C_1 S_1 & S_1 & 0 \\ C_1 C_1 & C_1 & 0 \\ C_1 & 0 & 0 \end{bmatrix},$$

and after that computing the controllability and observability matrices, both of them have three linearly independent rows and columns.

- Let N be an arbitrary positive integer number. For $N + 1$ matrices (33), (34) and (35) hold the same form that for N , only the dimensions of these matrices will be changed. Consequently, the same fact is valid for matrices $\mathcal{R}_{\mathbf{A}_M}, \mathbf{B}_M$ and $\mathcal{S}_{\mathbf{C}_M}, \mathbf{A}_M$. Therefore, if matrices $\mathcal{R}_{\mathbf{A}_M}, \mathbf{B}_M$ and $\mathcal{S}_{\mathbf{C}_M}, \mathbf{A}_M$ have $\eta(2N - 1)$ linearly independent rows and columns for N , they have $\eta(2(N + 1) - 1)$ linearly independent rows and columns for $N + 1$ (in $\eta, M = 2$).

¹ The mentioned values should be avoided because they have null sine or cosine values, which would correspond to zero-valued elements in the controllability and observability matrices. Therefore, the resulting matrices would not have full rank.

By the mathematical induction principle, it is demonstrated that matrices $\mathcal{R}_{\mathbf{A}_M}, \mathbf{B}_M$ and $\mathcal{S}_{\mathbf{C}_M}, \mathbf{A}_M$ have $\eta(2N - 1)$ linearly independent rows and columns. Thus, any realization $(\mathbf{A}_M, \mathbf{B}_M, \mathbf{C}_M, \mathbf{D}_M)$ (with all angles different from $0, \pi/2, \pi$ and $3\pi/2$) for $M = 2$ is minimal.

Theorem 2 A realization $(\mathbf{A}_M, \mathbf{B}_M, \mathbf{C}_M, \mathbf{D}_M)$ given by (29), (30), (31) and (32), respectively, with all angles different from $0, \pi/2, \pi$ and $3\pi/2$, is minimal because it is reachable and observable.

Proof By the mathematical induction principle and the following conclusions, the proof of the theorem is achieved as follows.

- For $M = 1$, it is demonstrated by Uzinski et al. (2015) that $\mathcal{R}_{\mathbf{A}_M}, \mathbf{B}_M$ and $\mathcal{S}_{\mathbf{C}_M}, \mathbf{A}_M$ have $\eta(2N - 1)$ linearly independent rows and columns (in $\eta, M = 1$).
- For $M = 2$, it is demonstrated by Lemma 1 that $\mathcal{R}_{\mathbf{A}_M}, \mathbf{B}_M$ and $\mathcal{S}_{\mathbf{C}_M}, \mathbf{A}_M$ have $\eta(2N - 1)$ linearly independent rows and columns (in $\eta, M = 2$).
- For any $M \geq 2$, the forms of $\mathbf{A}_M, \mathbf{B}_M$ and \mathbf{C}_M are the same as stated by (29), (30), (31) and (32), only the dimensions change according to M . The same fact is valid for the matrices $\mathcal{R}_{\mathbf{A}_M}, \mathbf{B}_M$ and $\mathcal{S}_{\mathbf{C}_M}, \mathbf{A}_M$. Therefore, if $\mathcal{R}_{\mathbf{A}_M}, \mathbf{B}_M$ and $\mathcal{S}_{\mathbf{C}_M}, \mathbf{A}_M$ have $\eta(2N - 1)$ linearly independent rows and columns, it implies that $\mathcal{R}_{\mathbf{A}_{M+1}}, \mathbf{B}_{M+1}$ and $\mathcal{S}_{\mathbf{C}_{M+1}}, \mathbf{A}_{M+1}$ have $\eta(2N - 1)$ (in η , the value of M is $M + 1$) linearly independent rows and columns.

By the mathematical induction principle, it is demonstrated that matrices $\mathcal{R}_{\mathbf{A}_M}, \mathbf{B}_M$ and $\mathcal{S}_{\mathbf{C}_M}, \mathbf{A}_M$ have $\eta(2N - 1)$ linearly independent rows and columns. Thus, any realization $(\mathbf{A}_M, \mathbf{B}_M, \mathbf{C}_M, \mathbf{D}_M)$ (with all angles different from $0, \pi/2, \pi$ and $3\pi/2$) is minimal.

Remark 1 When the designer considers that the dynamical system has a large number of states and for some reason it can be unsatisfactory, an order reduction method can be applied to the states \mathbf{x}_M of the description (29), (30), (31) and (32).

3 Proposed Dynamic-State Feedback Approach

3.1 Preliminaries: Discrete Linear Quadratic Regulator (DLQR)

Consider a plant described by a discrete-time model of the form

$$\mathbf{x}_p[k + 1] = \mathbf{A}_p \mathbf{x}_p[k] + \mathbf{B}_p \mathbf{u}_p[k], \tag{36}$$

where $\mathbf{x}_p[k] \in \mathbb{R}^n, \mathbf{u}_p[k] \in \mathbb{R}^p$ are the state and control vectors, and $\mathbf{A}_p, \mathbf{B}_p$ are matrices of compatible dimensions.

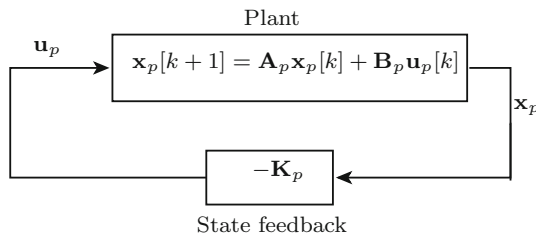


Fig. 7 Discrete linear quadratic regulator

It is assumed that the plant is controllable and the state $\mathbf{x}_p[k]$ is available for feedback.

Given the following quadratic cost function:

$$J = \sum_{k=0}^{\infty} \mathbf{x}_p^T[k] \mathbf{Q}_p \mathbf{x}_p[k] + \mathbf{u}_p^T[k] \mathbf{R}_p \mathbf{u}_p[k], \tag{37}$$

with positive-definite state and control weight matrices $\mathbf{Q}_p, \mathbf{R}_p$, the optimal control law is of the form

$$\mathbf{u}_p[k] = -\mathbf{K}_p \mathbf{x}_p[k], \tag{38}$$

with feedback gain \mathbf{K}_p calculated as

$$\mathbf{K}_p = (\mathbf{B}_p^T \mathbf{P} \mathbf{B}_p + \mathbf{R}_p)^{-1} \mathbf{B}_p^T \mathbf{P} \mathbf{A}_p, \tag{39}$$

where \mathbf{P} is the positive-definite solution of the following Riccati equation (Lewis 1986).

$$\mathbf{P} = \mathbf{A}_p^T \mathbf{P} \mathbf{A}_p - \mathbf{A}_p^T \mathbf{P} \mathbf{B}_p (\mathbf{R}_p + \mathbf{B}_p^T \mathbf{P} \mathbf{B}_p)^{-1} \mathbf{B}_p^T \mathbf{P} \mathbf{A}_p + \mathbf{Q}_p. \tag{40}$$

Fig. 7 shows the block diagram for the resulting control loop. As will be discussed in Sect. 4 (Case study), the weight matrices $\mathbf{Q}_p, \mathbf{R}_p$ can be adjusted in order to optimize a robustness or performance metric of interest.

3.2 Discrete Linear Quadratic Regulator Employing a Wavelet Filter Bank (DLQR-WFB)

In the DLQR-WFB approach proposed herein, a filter bank is included in the feedback path, as illustrated in Fig. 8. More specifically, each state of the plant is decomposed by the fast wavelet transform, in order to obtain an augmented state vector $\mathbf{x}_{pw} = [\mathbf{x}_p^T \ \mathbf{x}_w^T]^T$, with \mathbf{x}_w comprising the state variables of the filter bank. Since the fast wavelet transform is applied to each of the n components of the plant state \mathbf{x}_p , the filter bank state \mathbf{x}_w is formed as

$$\mathbf{x}_w = \begin{bmatrix} \mathbf{X}_{FB1} \\ \mathbf{X}_{FB2} \\ \vdots \\ \mathbf{X}_{FBn} \end{bmatrix}, \tag{41}$$

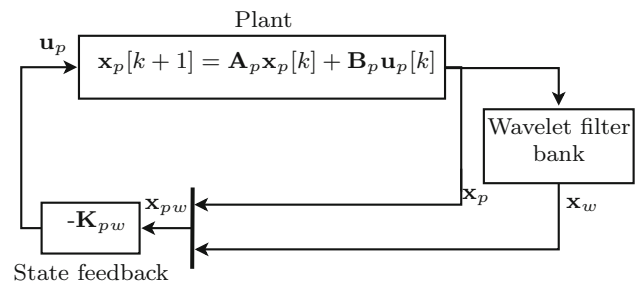


Fig. 8 Discrete linear quadratic regulator employing a wavelet filter bank

where \mathbf{x}_{FB_i} is a vector with the filter states involved in the decomposition of the i th plant state.

The dynamics of the plant coupled with the filter bank can then be described by a state equation of the form

$$\mathbf{x}_{pw}[k+1] = \mathbf{A}_{pw} \mathbf{x}_{pw}[k] + \mathbf{B}_{pw} \mathbf{u}_p[k], \tag{42}$$

where

$$\mathbf{x}_{pw}[k] = \begin{bmatrix} \mathbf{x}_p[k] \\ \mathbf{x}_w[k] \end{bmatrix}, \quad \mathbf{A}_{pw} = \begin{bmatrix} \mathbf{A}_p & 0 \\ \mathbf{B}_w & \mathbf{A}_w \end{bmatrix}, \tag{43}$$

$$\mathbf{B}_{pw} = \begin{bmatrix} \mathbf{B}_p \\ 0 \end{bmatrix},$$

with \mathbf{A}_w and \mathbf{B}_w obtained from the filter bank equations as

$$\mathbf{A}_w = \begin{bmatrix} \mathbf{A}_M & 0 & \cdots & 0 \\ 0 & \mathbf{A}_M & \cdots & 0 \\ \vdots & \vdots & \ddots & \vdots \\ 0 & 0 & \cdots & \mathbf{A}_M \end{bmatrix}, \quad \mathbf{B}_w = \begin{bmatrix} \mathbf{B}_M & 0 & \cdots & 0 \\ 0 & \mathbf{B}_M & \cdots & 0 \\ \vdots & \vdots & \ddots & \vdots \\ 0 & 0 & \cdots & \mathbf{B}_M \end{bmatrix}. \tag{44}$$

A discrete linear quadratic regulator with weight matrices $\mathbf{Q}_{pw}, \mathbf{R}_{pw}$ can be designed for the augmented system (42) in order to obtain a feedback gain \mathbf{K}_{pw} , as illustrated in Fig. 8.

4 Case Study

Consider a two-mass-spring system described by a continuous-time state equation of the form $\dot{\mathbf{x}}_p = \mathbf{A}_{pc} \mathbf{x}_p + \mathbf{B}_{pc} u_p$, with

$$\mathbf{A}_{pc} = \begin{bmatrix} 0 & 0 & 1 & 0 \\ 0 & 0 & 0 & 1 \\ -\frac{K_s}{m_{ac}} & \frac{K_s}{m_{ac}} & -\frac{b_{ac} + \frac{K_g^2 K_m K_t}{R_m r_{mp}^2}}{m_{ac}} & 0 \\ \frac{K_s}{m_{pc}} & -\frac{K_s}{m_{pc}} & 0 & -\frac{b_{pc}}{m_{pc}} \end{bmatrix}, \tag{45}$$

$$\mathbf{B}_{pc} = \begin{bmatrix} 0 & 0 & \frac{K_g K_t}{R_m r_{mp}} & 0 \end{bmatrix}^T,$$

Table 1 Model parameters

Parameter	Physical meaning	Value
K_s	Spring stiffness coefficient	142 N/m
m_{ac}	Active cart mass	1.15 kg
m_{pc}	Passive cart mass	0.54 kg
b_{ac}	Viscous friction coefficient (active cart)	5.4 Ns/m
b_{pc}	Viscous friction coefficient (passive cart)	2.2 Ns/m
K_g	Gearbox ratio	3.71
K_m	Counter-electromotive force constant	7.67×10^{-3} Vs/rad
K_t	Motor torque constant	7.67×10^{-3} Nm/A
R_m	Motor armature resistance	2.6 Ω
r_{mp}	Motor pinion radius	6.35 mm

with parameter values given in Table 1 (Colombo Junior et al. 2016). This model was discretized into the form (36) by using the zero-order hold method with a sampling period $T = 15$ ms, as in Colombo Junior et al. (2016).

In the present example, the proposed DLQR-WFB approach for dynamic-state feedback will be illustrated by using a db3 wavelet filter bank with $M = 2$ levels. This filter bank can be described by a state-space model with $\mathbf{A}_M, \mathbf{B}_M, \mathbf{C}_M, \mathbf{D}_M$ matrices as in (29), (30), (31), (32) where $\mathbf{A}, \mathbf{B}, \mathbf{C}, \mathbf{D}$ are given by (7), (8), (9), (10). The numerical values for the coefficients in $\mathbf{A}, \mathbf{B}, \mathbf{C}, \mathbf{D}$ can be found in Uzinski et al. (2015). By using a balanced realization and removing the states corresponding to small Hankel singular values (Laub et al. 1987), the model order for the filter bank was reduced from 15 to 10. It is worth noting that four separate filter banks will be employed in the control loop (one for each of the four plant states). Therefore, the overall order of the augmented system will be $4 + 10 + 10 + 10 + 10 = 44$.

In what follows, the DLQR (Fig. 7) and DLQR-WFB (Fig. 8) methods will be compared in two numerical investigations using different evaluation metrics.

The numerical results were obtained by using the Matlab® software, with the Optimization and Control System ToolboxesTM.

4.1 Sensitivity

Let $S(z)$ be a sensitivity function defined for the DLQR case as

$$S(z) = \frac{1}{1 + \mathbf{K}_p(z\mathbf{I} - \mathbf{A}_p)^{-1}\mathbf{B}_p}, \tag{46}$$

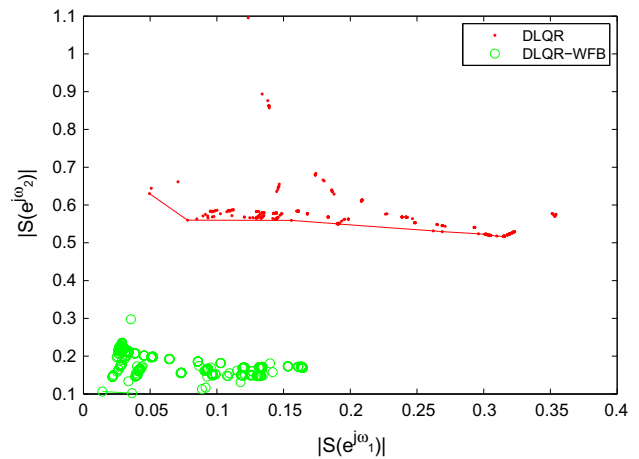


Fig. 9 Sensitivity values at $\omega_1 = 0.15$ and $\omega_2 = 0.60$ obtained by optimizing the state weights in the DLQR and DLQR-WFB formulations

with a similar definition in the DLQR-WFB case (replacing $\mathbf{K}_p, \mathbf{A}_p, \mathbf{B}_p$ with $\mathbf{K}_{pw}, \mathbf{A}_{pw}, \mathbf{B}_{pw}$, respectively) (Franklin et al. 1998).

This sensitivity function can be used as a robustness measure, since the value $|S(e^{j\omega})|$ is the reciprocal of the distance between the Nyquist curve and the critical point -1 , considering the loop broken at the plant input (Franklin et al. 1998). In this sense, a possible design goal may consist of obtaining small values of $|S(e^{j\omega})|$ at a given set of frequencies ω . This can be achieved by using a numerical optimization method to adjust the control and state weights in the DLQR or DLQR-WFB formulations.

In this example, diagonal weight matrices were adopted for simplicity. The control weight was set to one and a diagonal form was adopted for the state weight matrix, with diagonal elements optimized by using the sequential quadratic programming (SQP) method (Nocedal and Wright 2006). For this purpose, the fmincon function of the MATLAB Optimization ToolboxTM was employed, with default settings for the numerical search procedure. The weights corresponding to the four plant states were initialized by using 81 different combinations of the values $10^{-4}, 10^0$ and 10^4 . In the DLQR-WFB case, the weights corresponding to the filter bank states were initialized with null values. The index to be minimized was defined as $|S(e^{j\omega_1})| + \rho|S(e^{j\omega_2})|$, where $\omega_1 = 0.15, \omega_2 = 0.60$ and ρ is a positive scalar that can be adjusted to place larger emphasis on the minimization of $|S(e^{j\omega_1})|$ or $|S(e^{j\omega_2})|$.

Fig. 9 presents the DLQR and DLQR-WFB results obtained by varying the value of ρ . As can be seen, smaller values of $|S(e^{j\omega_1})|$ and $|S(e^{j\omega_2})|$ can be achieved by using the proposed DLQR-WFB formulation. Line segments connecting the non-dominated solutions (in the usual multi-objective sense) are included in the graphs, for better visualization.

4.2 Effect of External Disturbances and Measurement Noise

Consider the plant model (45) with a scalar output y_p defined as

$$y_p[k] = \mathbf{C}_p \mathbf{x}_p[k], \tag{47}$$

where \mathbf{C}_p is a row vector of compatible dimension. In the present example, the output will be defined as the first state variable, i.e., $\mathbf{C}_p = [1 \ 0 \ 0 \ 0]$.

Assume that a disturbance d is applied at the plant input. In the DLQR case, the effect of the disturbance on the plant output y_p can be evaluated by replacing (38) with

$$u_p[k] = -\mathbf{K}_p \mathbf{x}_p[k] + d[k]. \tag{48}$$

From (36), (47) and (48), a transfer function $H_{dy}(z)$ can be obtained as

$$H_{dy}(z) = \frac{Y_p(z)}{D(z)} = \mathbf{C}_p (z\mathbf{I} - \mathbf{A}_p + \mathbf{B}_p \mathbf{K}_p)^{-1} \mathbf{B}_p. \tag{49}$$

The effect of the disturbance on the plant output can then be evaluated in terms of the H_2 norm of $H_{dy}(z)$, which is defined as, (Bunse-Gerstner et al. 2010),

$$\|H_{dy}\|_2 = \sqrt{\frac{1}{2\pi} \int_0^{2\pi} |H_{dy}(e^{j\omega})|^2 d\omega}. \tag{50}$$

A similar transfer function can be obtained in the DLQR-WFB case, by replacing $\mathbf{K}_p, \mathbf{A}_p, \mathbf{B}_p$ and \mathbf{C}_p with $\mathbf{K}_{pw}, \mathbf{A}_{pw}, \mathbf{B}_{pw}$ and $[\mathbf{C}_p \ 0]$, respectively.

Now, instead of considering an input disturbance, assume that the state values employed in the feedback control law are corrupted with a measurement noise term n such that

$$u_p[k] = -\mathbf{K}_p (\mathbf{x}_p[k] + \mathbf{E}_p n[k]) \tag{51}$$

in the DLQR case, where \mathbf{E}_p is a column vector of compatible dimension. In the present example, the noise will be included in the measurement of the first state variable, i.e., $\mathbf{E}_p = [1 \ 0 \ 0 \ 0]^T$. From (36), (47) and (51), a transfer function $H_{ny}(z)$ can be obtained as

$$H_{ny}(z) = \frac{Y_p(z)}{N(z)} = -\mathbf{C}_p (z\mathbf{I} - \mathbf{A}_p + \mathbf{B}_p \mathbf{K}_p)^{-1} \mathbf{B}_p \mathbf{K}_p \mathbf{E}_p. \tag{52}$$

The H_2 norm of $H_{ny}(z)$ can then be used to evaluate the effect of the measurement noise on the plant output. A similar transfer function can be obtained in the DLQR-WFB case,

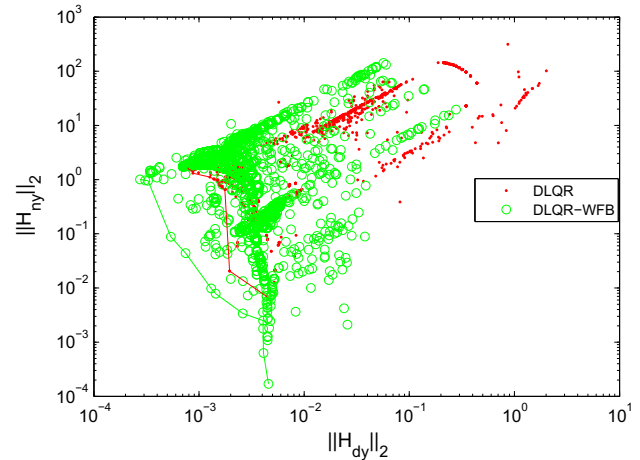


Fig. 10 Comparative evaluation of the DLQR and DLQR-WFB formulations in terms of external disturbance and measurement noise effects

by replacing $\mathbf{K}_p, \mathbf{A}_p, \mathbf{B}_p, \mathbf{C}_p$ and \mathbf{E}_p with $\mathbf{K}_{pw}, \mathbf{A}_{pw}, \mathbf{B}_{pw}, [\mathbf{C}_p \ 0]$ and $[\mathbf{E}_p^T \ 0]^T$, respectively.

As in the sensitivity study presented in Sect. 4.1, the state weights in the DLQR and DLQR-WFB formulations were optimized by using the SQP method. In this case, the index to be minimized was defined as $\|H_{dy}\|_2 + \rho \|H_{ny}\|_2$. Fig. 10 presents the DLQR and DLQR-WFB results obtained by varying the value of ρ . Again, the proposed DLQR-WFB approach leads to better results, in that smaller values of $\|H_{dy}\|_2$ and $\|H_{ny}\|_2$ can be achieved as compared to the DLQR formulation.

5 Conclusions

This paper presented a new state-space description for wavelet filter banks (WFBs) with multiple decomposition levels, thus extending previous work on single-level decomposition schemes. The proposed description can be used to design dynamic-state feedback control laws involving the decomposition of the plant states by the filter bank. A simple synthesis procedure consists of designing a discrete linear quadratic regulator (DLQR) for the augmented system incorporating the plant model and the filter bank.

A numerical example was presented to illustrate the potential advantages of the proposed DLQR-WFB approach. For this purpose, a standard DLQR design was employed for comparison. As a result, the proposed approach was shown to provide better results in terms of sensitivity values, as well as rejection of external disturbances and measurement noise.

Future research could be concerned with the development of guidelines for choosing the type of wavelet and the number of decomposition levels in view of the design requirements

for the closed-loop system. The use of WFBs with control design methods other than DLQR could also be investigated.

Acknowledgements The authors acknowledge the support of the Brazilian agencies CAPES, CNPq (research fellowships and Ph.D. Grant 160545/2013-7) and FAPESP (Grant 2011/17610-0).

References

- Akansu, A. N., & Haddad, R. A. (2001). *Multiresolution signal decomposition: Transforms, subbands, and wavelets*. San Diego: Academic Press.
- Bunse-Gerstner, A., Kubaliska, D., Vossen, G., & Wilczek, D. (2010). h_2 -norm optimal model reduction for large scale discrete dynamical MIMO systems. *Journal of Computational and Applied Mathematics*, 233(5), 1202–1216.
- Colombo Junior, J. R., Afonso, R. J. M., Galvão, R. K. H., & Assunção, E. (2016). Robust model predictive control of a benchmark electromechanical system. *Journal of Control, Automation and Electrical Systems*, 27(2), 119–131.
- Fernando, W. U. N., & Kumarawadu, S. (2015). Discrete-time neuroadaptive control using dynamic state feedback with application to vehicle motion control for intelligent vehicle highway systems. *IET Control Theory and Applications*, 4(8), 1465–1477.
- Franklin, G. F., Powell, J. D., & Workman, M. (1998). *Digital control of dynamic systems*. Menlo Park: Addison Wesley Longman.
- Holmberg, U., Fu, M., & Zhang, C. (2001). Comments on “A revisit to the gain and phase margins of linear quadratic regulators” [with reply]. *IEEE Transactions on Automatic Control*, 46(9), 1508–1509.
- Laub, A. J., Heath, M. T., Paige, C. C., & Ward, R. C. (1987). Computation of system balancing transformations and other applications of simultaneous diagonalization algorithms. *IEEE Transactions on Automatic Control*, 32(2), 115–122.
- Lewis, F. L. (1986). *Optimal control*. New York: John Wiley & Sons.
- Liu, H., Lu, G., & Zhong, Y. (2013). Robust LQR attitude control of a 3-DOF laboratory helicopter for aggressive maneuvers. *IEEE Transactions on Industrial Electronics*, 60(10), 4627–4636.
- Lublin, L., & Athans, M. (1996). Linear quadratic regulator control. In W. S. Levine (Ed.), *The control handbook* (1st ed., pp. 635–650). Boca Raton: CRC Press.
- Maccari, L. A., Santini, C. L. A., Oliveira, R. C. L. F., & Montagner, V. F. (2014). Design and experimental implementation of a robust DLQR for three-phase grid-connected converters. In: *IEEE/IAS international conference on industry applications (INDUSCON) (2014)*, Juiz de Fora, Brazil (pp. 1–6).
- Nocedal, J., & Wright, S. J. (2006). *Numerical optimization*. New York: Springer.
- Paiva, H. M. (2005). *Wavelet-packet identification of dynamic systems in frequency subbands*. Ph.D. thesis, Instituto tecnológico de aeronáutica—ITA, São José dos Campos, SP, Brazil. Available on: http://www.bdiita.bdiita.br/tesesdigitais/lista_resumo.php?num_tese=000540721.
- Paiva, H. M., & Galvão, R. K. H. (2012). Optimized orthonormal wavelet filters with improved frequency separation. *Digital Signal Processing*, 22(4), 622–627.
- Paiva, H. M., Martins, M. N., Galvão, R. K. H., & Paiva, J. (2009). On the space of orthonormal wavelets: additional constraints to ensure two vanishing moments. *IEEE Signal Processing Letters*, 16(2), 101–104.
- Pradhan, J. K., & Ghosh, A. (2015). Multi-input and multi-output proportional-integral-derivative controller design via linear quadratic regulator-linear matrix inequality approach. *IET Control Theory and Applications*, 9(14), 2140–2145.
- Schmitendorf, W. E., & Stalford, H. L. (1997). Improving stability margins via dynamic-state feedback for systems with constant uncertainty. *IEEE Transactions on Automatic Control*, 42(8), 1161–1163.
- Sherlock, B. G., & Monro, D. M. (1998). On the space of orthonormal wavelets. *IEEE Transactions on Signal Processing*, 46(6), 1716–1720.
- Ulsoy, A. G. (2013). Improving stability margins via time delay control. In *ASME 2013 international design engineering technical conferences and computers and information in engineering conference*, Oregon, Portland (pp. 1–10).
- Ulsoy, A. G. (2015). Time-delayed vibration control of two degree-of-freedom mechanical system for improved stability margins. In *12th IFAC workshop on time delay systems TDS*, Michigan, USA : Ann Arbor, (pp. 1–6).
- Uzinski, J. C., Paiva, H. M., Duarte, M. A. Q., Galvão, R. K. H., & Villarreal, F. (2015). A state-space description for perfect-reconstruction wavelet FIR filter banks with special orthonormal basis functions. *Journal of Computational and Applied Mathematics*, 290, 290–297.
- Vaidyanathan, P. P. (1993). *Multirate systems and filter banks*. New Jersey: Prentice Hall.
- Verdea, C., Rojas, J. L. A., & Fuente-Esquivel, C. R. (2013). Improving stability margin in electric power systems by linear quadratic regulator and disturbance model. *Electric Power Components and Systems*, 41(14), 1415–1431.
- Vetterli, M., & Kovačević, J. (1995). *Wavelets and subband coding*. New Jersey: Prentice Hall.
- Zhang, C., & Fu, M. (1996). A revisit to the gain and phase margins of linear quadratic regulators. *IEEE Transactions on automatic control*, 41(10), 1527–1530.
- Zhang, R., Zhixing, C., Ping, L., & Furong, G. (2014). Design and implementation of an improved linear quadratic regulation control for oxygen content in a coke furnace. *IET Control Theory and Applications*, 8(14), 1303–1311.